Adaptive Nulling Through Subarray Switching in Planar Antenna Arrays

M. Salucci[(1)(2)], L. Poli[(1)], A. F. Morabito[(3)], and P. Rocca[(1)]

[(1)] *ELEDIA Research Center @ DISI*

University of Trento, Via Sommarive 5, 38123 Trento - Italy

Tel. +39 0461 282057, Fax +39 0461 283166

E-mail: {*marco.salucci*, *lorenzo.poli*, *paolo.rocca*}*@unitn.it*

Web-site: *http://www.eledia.ing.unitn.it*

[(2)] *ELEDIA Offshore Lab @ Paris*

Laboratoire des Signaux et Systèmes (L2S, UMR CNRS 8506), 3 rue Joliot Curie,

91192 Gif-sur-Yvette, France

E-mail: {*marco.salucci*}*@l2s.centralesupelec.fr*

[(3)] LEMMA Research Group @ *DIIES*

University of Reggio Calabria, Località Feo di Vito, 89060 Reggio Calabria - Italy

Tel. +39 0965 875262, Fax +39 0965 875220

E-mail: *andrea.morabito@unirc.it*

This is the post-print of the following article: M. Salucci, L. Poli, A.F. Morabito, and P. Rocca "Adaptive nulling through subarray switching in planar antenna arrays," Journal of Electromagnetic Waves and Applications, vol. 30, n. 3, pp. 404-414, 2016.
Article has been published in final form at: https://www.tandfonline.com/doi/full/10.1080/09205071.2015.1130662.
DOI: 10.1080/09205071.2015.1130662.

Adaptive Nulling Through Subarray Switching in Planar Antenna Arrays

M. Salucci, L. Poli, A. F. Morabito, and P. Rocca

Abstract

The suppression of undesired signals impinging on a planar antenna array from unknown directions is addressed by adaptively connecting and disconnecting subarrays of elements from the beamforming network. The subarrays, periodically arranged on the array aperture, are equipped with radio-frequency switches that are controlled to maximize the ratio between the power of the desired signal, whose direction of arrival is supposed to be known, and the total power received by the antenna. A set of numerical results concerning different subarray layouts and interfering configurations is reported and discussed to show the effectiveness of the nulling method and the behavior of the considered array architectures.

Key words: Pattern Nulling, Adaptive Arrays, Subarraying, Genetic Algorithms.

1 Introduction

The rapid congestion of the wireless spectrum due to the great diffusion of mobile services has raised the attention towards reconfigurable antennas which allow to correctly receive desired signals while suppressing the interfering ones [1]. The basic idea is to adaptively tune the antenna control points in order to place nulls or deep sidelobes in the beam pattern in correspondence with the directions of arrival (DoAs) of the interferences and maintain the main lobe along the DoA of the desired one. Thanks to the high number of control points (e.g., amplifiers, phase shifters), phased antenna arrays have been effectively exploited for pattern nulling [2] and widely used in both radar and communication applications.

Several methodologies for the adaptive control of phase arrays have been proposed in the scientific literature. In [3], nulls in the far-field pattern have been generated along the DoAs of the interfering signals through the synthesis of suitable complex weighting coefficients. The method is based on the multiplication of the quiescent element weights (i.e., those used in the noise-free case) by the inverse of the covariance matrix computed from the signals received at the output of the array elements. Although the achievable optimal nulling performance, this strategy has shown to be impractical due to the high costs of the hardware implementation because a receiver is required for each element of the array. Successively, phase-only adaptive techniques have been introduced [4][5][6][7]. In this case, the nulls in the radiation pattern are generated by only changing the phases of the excitations while the amplitude values are kept fixed. Among these latter, an approach based on a binary Genetic Algorithm (GA) has been proposed to adjust the least significant bits of the digital phase shifters such to obtain deep nulls in the interference directions while slightly perturbing the beam steering direction as well as the sidelobe level [7]. Whether on the one hand the optimization of only few bits has allowed to reduce the number of problem unknowns and improve the GA convergence speed, on the other hand good nulling performance across the whole secondary lobe region can be only achieved with arrays having many elements. In the last years, several other approaches based on biologically inspired optimization algorithms have shown effective results in dealing with the pattern nulling problem [8][9][10][11][12]. In such cases, the main issue is the efficiency of the algorithms in converging to a reliable solution, possibly the one providing the best

nulling performance. As a matter of fact, the number of trial solutions (i.e., the cardinality of the solution space) grows exponentially with the number of array elements thus limiting the fast convergence to the optimal excitations setting in case of medium and large arrays. In order to overcome this problem, an advanced methodology has been proposed in [13] where the reaction time of the Particle Swarm Optimizer (PSO) has been reduced through a memory-based strategy. More specifically, a database of optimized solutions obtained from previously addressed interfering scenarios is stored and used in order to initialize the PSO-based optimization step when addressing a new nulling problem.

A different approach based on a simplified array architecture has been considered in [14][15] where a set of radio-frequency (RF) switches has been adopted to either connect or disconnect the elements of a linear array from the beam-forming network (BFN) with the aim of shaping the beam pattern and reducing the power of the interfering signals. The array elements are activated/deactivated according to a set of pre-defined binary sequences and the one providing the best signal-to-noise-plus-interference ratio ($SINR$) performance is maintained until a decrement of the signal quality is measured [14]. Differently, the direct optimization of a metric proportional to the $SINR$ has been carried out in [15] by means of a binary GA which allowed to achieve better nulling performance as compared to [14] at the cost of the increment of the reaction time. Although the on-off control requires the optimization of just a single bit for each array element, also in this case the number of possible switching configurations is extremely wide when many elements are present in the array thus preventing the real-time or almost real-time optimization.

In this work, an innovative array architecture is taken into account in which the array is partitioned into sub-arrays and one RF switch is used for each cluster of two or more elements. The binary GA is used to optimize the on-off status of the switches at the subarray level. The performance of the proposed approach is numerically validated against single and multiple interference scenarios when considering different partitionings of the planar array aperture into subarrays.

The remaining of the paper is organized as follows. The nulling problem is mathematically formulated in Sect. 2, where the binary GA approach is described. A set of numerical results

is reported in Sect. 3 in order to validate the effectiveness of the proposed solution. Eventually, some conclusions are drawn (Sect. 4).

2 Mathematical Formulation

Let us consider a planar array made of $M \times N$ elements disposed on a rectangular lattice in the xy plane. The elements are clustered into Q equal subarrays periodically distributed on the antenna aperture. Each subarray is equipped with a RF switch [Fig. 1(a)] which allows to either connect ($\alpha_q = 1$) or disconnect ($\alpha_q = 0$) the radiating elements from the BFN. Accordingly, the array factor of the antenna can be mathematically expressed as

$$AF\left(\theta,\phi\right) = \frac{1}{\xi_{on}} \sum_{q=1}^{Q} \alpha_q \sum_{m=1}^{M} \sum_{n=1}^{N} \delta_{c_{mn}q} e^{j\left(\Phi_{mn}\left(\theta,\phi\right)+\varphi_{mn}\right)} \tag{1}$$

where

$$\Phi_{mn}\left(\theta,\phi\right) = \beta\left[\left(m-1\right)d_x \sin\theta\cos\phi + \left(n-1\right)d_y \sin\theta\sin\phi\right] \tag{2}$$

is the phase term depending from the position $(x_{mn},\, y_{mn})$ of the mn-th element [i.e., $x_{mn} = \left(m-1\right)d_x$ and $y_{mn} = \left(n-1\right)d_y$] and the angular direction (θ,ϕ), d_x and d_y the inter-element distance along the x-axis and y-axis, respectively, $\beta = \frac{2\pi}{\lambda}$ the wave number, λ being the free space wavelength. Moreover, φ_{mn}, $m = 1, ..., M$, $n = 1, ..., N$ are the excitation phases which are used for the beam steering and $\delta_{c_{mn}q}$ the Kronecker delta equal to $\delta_{c_{mn}q} = 1$ when $c_{mn} = q$ and $\delta_{c_{mn}q} = 0$, otherwise. The integer values $c_{mn} \in [1 : Q]$, $m = 1, ..., M$, $n = 1, ..., N$ identify the membership of each element to a subarray. The normalization coefficient in (1) is defined as

$$\xi_{on} = \sum_{q=1}^{Q} \alpha_q \sum_{m=1}^{M} \sum_{n=1}^{N} \delta_{c_{mn}q} \tag{3}$$

and is equal to the number of active elements, namely the number of elements belonging to the subarrays with $\alpha_q = 1$ ($q = 1, ..., Q$).

A set of U undesired signals modeled as narrow-band plane waves s_u, $u = 1, ..., U$ are supposed arriving on the planar array from unknown DoAs (θ_u, ϕ_u), $u = 1, ..., U$. The DoA of the desired signal s_d is instead known and equal to (θ_d, ϕ_d). Because the array is equipped with a single

receiver after the power combiner [Fig. 1(a)], only the total power $\mathcal{P}_{TOT}$ can be measured at the antenna output, namely the quantity

$$\mathcal{P}_{TOT}\left(\underline{\alpha}\right) = \mathcal{P}_{d}\left(\underline{\alpha}\right) + \sum_{u=1}^{U} \mathcal{P}_{u}\left(\underline{\alpha}\right) + \mathcal{P}_{n} \tag{4}$$

where $\underline{\alpha} = \{\alpha_q : \ q = 1, ..., Q\}$. In (4), the term $\mathcal{P}_d$ is the power associated to the desired signal

$$\mathcal{P}_{d}\left(\underline{\alpha}\right) = \left| s_d \sum_{q=1}^{Q} \alpha_q \sum_{m=1}^{M} \sum_{n=1}^{N} \delta_{c_{mnq}} e^{j(\Phi_{mn}(\theta_d,\phi_d)+\varphi_{mn})} \right|^2 \tag{5}$$

and $\mathcal{P}_u$ is the power collected by the antenna from the u-th interference

$$\mathcal{P}_{u}\left(\underline{\alpha}\right) = \left| s_u \sum_{q=1}^{Q} \alpha_q \sum_{m=1}^{M} \sum_{n=1}^{N} \delta_{c_{mnq}} e^{j(\Phi_{mn}(\theta_u,\phi_u)+\varphi_{mn})} \right|^2 , u = 1, ..., U. \tag{6}$$

Moreover, $\mathcal{P}_n$ is the power of the background noise, modeled as a Gaussian process with zero mean and variance $\mathcal{P}_n$. Since the signal-to-noise-plus-interference ratio

$$SINR\left(\underline{\alpha}\right) = \frac{\mathcal{P}_{d}\left(\underline{\alpha}\right)}{\sum_{u=1}^{U} \mathcal{P}_{u}\left(\underline{\alpha}\right) + \mathcal{P}_{n}} \tag{7}$$

is a quantity that can not be directly obtained from antenna measurements (i.e., it is not possible to distinguish the power contributions of the desired and undesired signals), the on-off sequence is optimized such to maximize the following metric

$$\Psi\left(\underline{\alpha}\right) = \frac{\mathcal{P}_{d}\left(\underline{\alpha}\right)}{\mathcal{P}_{TOT}\left(\underline{\alpha}\right)} \tag{8}$$

that is directly proportional to the $SINR$ and has the same global optimum [16]. Unlike (7), the function (8) is measurable for a given setting of the RF switches. As a matter of fact, the numerator can be estimated through (5) once (θ_d, ϕ_d) is known while the value of the denominator can be directly measured at the antenna output.

The optimization of (8) is carried out by means of a binary GA according to the procedure described in the flowchart of Fig. 2, where I is the number of individuals of the GA population, p_c and p_m the probability of applying the crossover and the mutation operators, respectively,

and K_{stop} a maximum number of iterations defined by the user in order to stop the optimization process [17].

3 Numerical Assessment

The proposed approach based on subarrayed adaptive nulling is validated in this section by considering a set of representative numerical examples characterized by different electromagnetic scenarios as well as array layouts (Fig. 3). More in details, clusters of two elements (i.e., $Q = Q_2 = \frac{M \times N}{2}$) with one [Fig. 3(*a*) - Q_2^H] or two orientations [Fig. 3(*b*) - Q_2^{HV}] as well as four elements (i.e., $Q = Q_4 = \frac{M \times N}{4}$) [Fig. 3($c$)] are taken into account and compared in terms of pattern nulling performance.

As a representative benchmark antenna, a square array composed of 144 elements ($M = N = 12$) with $d_x = d_y = \frac{\lambda}{2}$ has been considered. In all simulations, the DoA of the desired signal has been fixed at broadside, namely $(\theta_d, \phi_d) = (0, 0)$, [i.e., $(u_d, v_d) = (0, 0)$, being $u = \sin\theta\cos\phi$ and $v = \sin\theta\sin\phi$]. Moreover, the power of the interfering signals $|s_u|^2$, $u = 1, ..., U$ has been set to $+30\,dB$ with respect to $|s_d|^2$ while $P_n = -30\,dB$. The setting of the GA control parameters (Fig. 2) has been chosen according to the guidelines of [17] ($P = \frac{Q}{2}$, $p_c = 0.9$, $p_m = 0.01$) while the maximum number of iterations has been fixed to $K_{stop} = 200$ in order to guarantee the convergence of the optimization process in less than one second considering the use of a standard computational resource (i.e., laptop PC $2.4GHz$ CPU and $2GB$ of RAM) as discussed in [15].

In the first test case (*Example 1*), the interference is arriving on the array from direction $(\theta_1, \phi_1) = (75°, 88°)$ [i.e., $(u_1, v_1) = (0.03, 0.97)$]. For each subarray configuration (Fig. 3), $T = 100$ simulations have been run starting from different initial populations at the first iteration ($k = 0$) because of the stochastic behavior of the GA. The average (avg), variance (var), minimum (min), and maximum (max) values of the $SINR$ for the best solutions achieved at the end of each GA run are reported in Tab. I together with the statistics of the null depth along the DoA of the interference. The results obtained when considering a fully-populated array configuration with one RF switch for each element of the array [i.e., $Q_{full} = M \times N$ - Fig. 1(*b*)] are reported as well. It is worth noting that the best average $SINR$ performance are obtained for the case Q_2^{HV}

(i.e., $avg\{SINR\}|_{Q_2^{HV}} = 47.05\,dB$). The average performance of the other subarray configurations are $10\,dB$ ($avg\{SINR\}|_{Q_2^{H}} = 37.54\,dB$) and $15\,dB$ ($avg\{SINR\}|_{Q_4} = 31.62\,dB$) worse. It is also important to observe how the average $SINR$ of the fully-populated configuration is $7\,dB$ lower ($avg\{SINR\}|_{Q_{full}} = 40.01\,dB$) than those achieved by the Q_2^{HV} layout. Although the larger number of degrees of freedom when $Q = Q_{full} = M \times N$ (i.e., there are no subarrays), it has been shown that the GA is not able to effectively sample the solution space whose dimension is much wider with respect to the subarray cases. Similar conclusions hold true when analyzing the data regarding the null depth values $|AF(\theta_1, \phi_1)|^2$ as shown in Tab. I. The solutions providing the maximum $SINR$ values among the $T = 100$ runs for each subarray configuration are shown in Fig. 4. More specifically, the on-off configuration of the array elements [Fig. 4(*a*), 4(*c*), 4(*e*), and 4(*g*)] and the corresponding power patterns [Fig. 4(*b*), 4(*d*), 4(*f*), and 4(*h*)] are given for the case with subarrays having two elements and a single orientation [Q_2^H: Fig. 4(*a*) and Fig. 4(*b*)] as well as two orientations [Q_2^{HV}: Fig. 4(*c*) and Fig. 4(*d*)], linear subarrays with four elements [Q_4: Fig. 4(*e*) and Fig. 4(*f*)], and the fully-populated configuration [Q_{full}: Fig. 4(*g*) and Fig. 4(*h*)]. In the pictures showing the status of the RF switches, the elements that are on and off are indicated with a black and a white pixel, respectively.

In the second test case (***Example 2***), two interferences arrive on the array from DoAs equal to $(\theta_1, \phi_1) = (75°, 88°)$ [i.e., $(u_1, v_1) = (0.03, 0.97)$] and $(\theta_2, \phi_2) = (-48°, 40°)$ [i.e., $(u_2, v_2) = (-0.57, -0.48)$], respectively. The statistical analysis of the GA behavior has been carried as in the previous example and also in this case the best average performance (Tab. II) are obtained for the two-element subarray layout with two orientations ($avg\{SINR\}|_{Q_2^{HV}} = 20.43\,dB$). It is worth to note that the presence of one more interference closer to the main lobe has caused a non-negligible and unavoidable reduction of the $SINR$ performance of almost $27\,dB$ ($avg\{SINR\}|_{Q_2^{HV}}^{U=1} = 47.05\,dB$ vs. $avg\{SINR\}|_{Q_2^{HV}}^{U=2} = 20.43\,dB$) and that the $SINR$ performance for the different array configurations are closer with a maximum deviation of almost $3dB$ (Tab. II). The worst $SINR$ performance among the $T = 100$ simulations has been achieved for the case Q_2^H ($min\{SINR\}|_{Q_2^H} = 12.35\,dB$). Such a $SINR$ value, still higher that $10\,dB$, demonstrates the capability of the proposed GA-based approach in effectively re-

configuring the array in order to suppress the undesired signals whatever the organization of the array elements into subarrays. As for the null depths along the DoAs of the two interferences, nulls lower than $-50\,dB$ with respect to the peak of the main beam have been obtained. Also in this case, the worst result guarantees a suppression of the interferences of at least $43\,dB$. For the sake of completeness, the on-off configuration of the array elements and the corresponding power patterns of the best solutions for the four subarray layouts are shown in Fig. 5.

As far as the computation time is concerned, the simulations based on sub-arrayed layouts have required an average run time, using a non-optimized code, of $0.020\,[sec]\rfloor_{Q_4}$ and $0.063\,[sec]\rfloor_{Q_2}$ while $0.112\,[sec]\rfloor_{Q_{full}}$ has been needed for the fully-populated array configurations.

4 Conclusions

The pattern nulling of planar antenna arrays composed of periodic sub-arrays has been addressed in this work. Each sub-array, equipped with a RF switch, has been connected or disconnected from the feeding network by means of a binary GA optimization technique in order to maximize the strength/quality of the desired signal on receive by creating nulls or deep sidelobes in the radiation pattern along the DoAs of the interferences. The reported numerical validation has shown:

- the effectiveness of the GA-based subarrayed adaptive nulling strategy in suppressing undesired signals with unknown DoAs;
- the superior performance achieved by subarrayed solutions as compared to the fully-populated array by virtue of the large reduction of the solution space cardinality, thus increasing the probability of retrieving an array configuration guaranteeing a better nulling;
- that the array architecture providing the best results is the one with subarrays made of the two elements and having two different orientations (i.e., Q_2^{HV});
- the efficiency of the adaptive strategy in reconfiguring the switching configuration of the subarrays.

Acknowledgements

This work benefited from the networking activities carried out within the *SIRENA* project (2014-2017) funded by *DIGITEO* (France) under the "Call for Chairs 2014".

References

[1] Godara, L. C.: 'Smart Antennas' (London, UK: CRC Press, 2004)

[2] Widrow, B., Mantey, P. E., Griffiths, L. J., Goode, B. B.: 'Adaptive antenna systems,' *IEEE Proc.*, 1967, **55**, (12), pp. 2143- 2159

[3] Applebaum, S. P.: 'Adaptive arrays,' *IEEE Trans. Antennas Propag.*, 1976, **24**, (5), pp. 585-598

[4] Baird, C. A., Rassweiler, G. G.: 'Adaptive sidelobe nulling using digitally controlled phase-shifters,' *IEEE Trans. Antennas Propag.*, 1976, **24**, (5), pp. 638-649

[5] Steyskal, H.: 'Simple method for pattern nulling by phase perturbation,' *IEEE Trans. Antennas Propag.*, 1983, **31**, (1), pp. 163-166

[6] Smith, S.T.: 'Optimum phase-only adaptive nulling,' *IEEE Trans. Signal Proc.*, 1999, **47**, (7), pp. 1835-1843

[7] Haupt, R. L.: 'Phase-only adaptive nulling with a genetic algorithm,' *IEEE Trans. Antennas Propag.*, 1997, **45**, (6), pp. 1009-1015

[8] Rajo-Iglesias E., Quevedo-Teruel, O.: 'Linear array synthesis using an ant-colony-optimization-based algorithm,' *IEEE Antennas Propag. Mag.*, 2007, **49**, (2), pp. 70-79

[9] Aksoy, E., Afacan, E.: 'Planar antenna pattern nulling using differential evolution algorithm,' *Int. J. Electron. Commun.*, 2009, **63**, (2), pp. 116-122

[10] Chen, Y., Yang, S., Li, G., Nie, Z.: 'Adaptive nulling with time-modulated antenna arrays using a hybrid differential evolution strategy,' *Electromagn.*, 2010, **30**, (7), pp. 574-588

[11] Goudos, S. K., Moysiadou, V., Samaras, T., Siakavara, K., Sahalos, J. N.: 'Application of a comprehensive learning particle swarm optimizer to unequally spaced linear array synthesis with sidelobe level suppression and null control,' *IEEE Antennas Wireless Propag. Lett.*, 2010, **9**, pp. 125-129

[12] Poli, L., Rocca, P., Oliveri, G., Massa, A.: 'Adaptive nulling in time- modulated linear arrays with minimum power losses,' *IET Microw. Antennas Propag.*, 2011, **5**, (2), pp. 157-166

[13] Benedetti, M., Azaro, R., Massa, A.: 'Memory enhanced PSO-based optimization approach for smart antennas control in complex interference scenarios,' *IEEE Trans. Antennas Propag.*, 2008, **56**, (7), pp. 1939-1947

[14] Rocca, P., Haupt, R. L., Massa, A.: 'Interference suppression in uniform linear arrays through a dynamic thinning strategy,' *IEEE Trans. Antennas Propag.*, 2011, **59**, (12), pp. 4525-4533

[15] Poli, L., Rocca, P., Salucci, M., Massa, A.: 'Reconfigurable thinning for the adaptive control of linear arrays,' *IEEE Trans. Antennas Propag.*, 2013, **61**, (10), pp. 5068-5077

[16] Weile D. S., Michielssen, E.: 'The control of adaptive antenna arrays with genetic algorithms using dominance and diploidy,' *IEEE Trans. Antennas Propag*., 2001, **49**, (10), pp. 1424-1433

[17] Rocca, P., Benedetti, M., Donelli, M., Franceschini, D., Massa, A.: 'Evolutionary optimization as applied to inverse scattering problems,' *Inv. Prob.*, 2009, **24**, pp. 1-41

FIGURE CAPTIONS

- **Figure 1.** Sketch of the antenna array architecture (*a*) with and (*b*) without subarrays.
- **Figure 2.** Flowchart of the GA-based optimization algorithm.
- **Figure 3.** Sketch of the subarray configuration having two elements and one orientation [Fig. 3(*a*) - Q_2^H], two orientations [Fig. 3(*b*) - Q_2^{HV}], and four elements [Fig. 3(*c*) - Q_4].
- **Figure 4.** *Example 1* - [$M = N = 12$, $d_x = d_y = \frac{\lambda}{2}$, $U = 1$] - Plot of the (*a*)(*c*)(*e*)(*g*) on-off subarray configuration and (*b*)(*d*)(*f*)(*h*) power pattern for the optimal solution obtained by means of the adaptive GA-based method for the subarrayed case (*a*)(*b*) Q_2^H, (*c*)(*d*) Q_2^{HV}, and (*e*)(*f*) Q_4, and (*g*)(*h*) the fully populated array (Q_{full}).
- **Figure 5.** *Example 2* - [$M = N = 12$, $d_x = d_y = \frac{\lambda}{2}$, $U = 2$] - Plot of the (*a*)(*c*)(*e*)(*g*) on-off subarray configuration and (*b*)(*d*)(*f*)(*h*) power pattern for the optimal solution obtained by means of the adaptive GA-based method for the subarrayed case (*a*)(*b*) Q_2^H, (*c*)(*d*) Q_2^{HV}, and (*e*)(*f*) Q_4, and (*g*)(*h*) the fully populated array (Q_{full}).

TABLE CAPTIONS

- **Table I.** *Example 1* - [$M = N = 12$, $d_x = d_y = \frac{\lambda}{2}$, $U = 1$] - $SINR$ and null depth $|AF(\theta_1, \phi_1)|^2$ statistics.
- **Table II.** *Example 2* - [$M = N = 12$, $d_x = d_y = \frac{\lambda}{2}$, $U = 2$] - $SINR$ and null depth $|AF(\theta_u, \phi_u)|^2$, $u = 1, 2$ statistics.

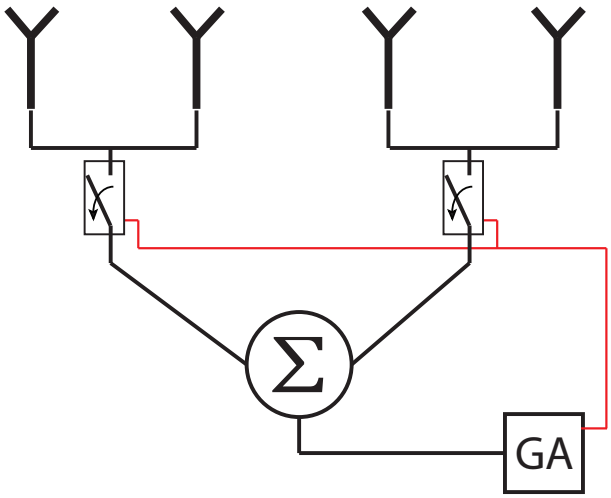

(a)

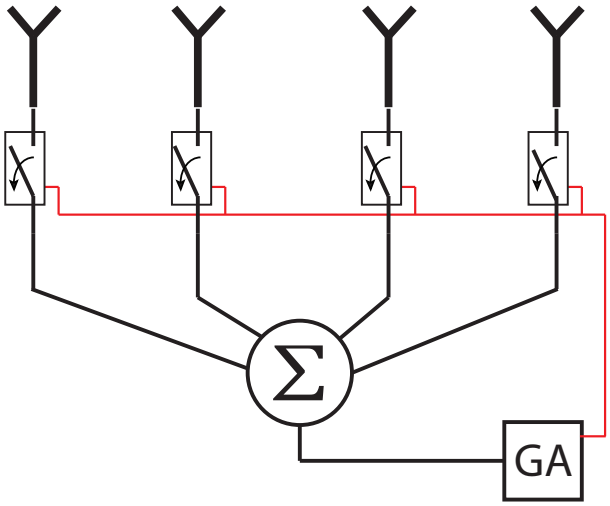

(b)

Fig. 1 - M. Salucci *et al.,* "Adaptive Nulling Through Subarray Switching ..."

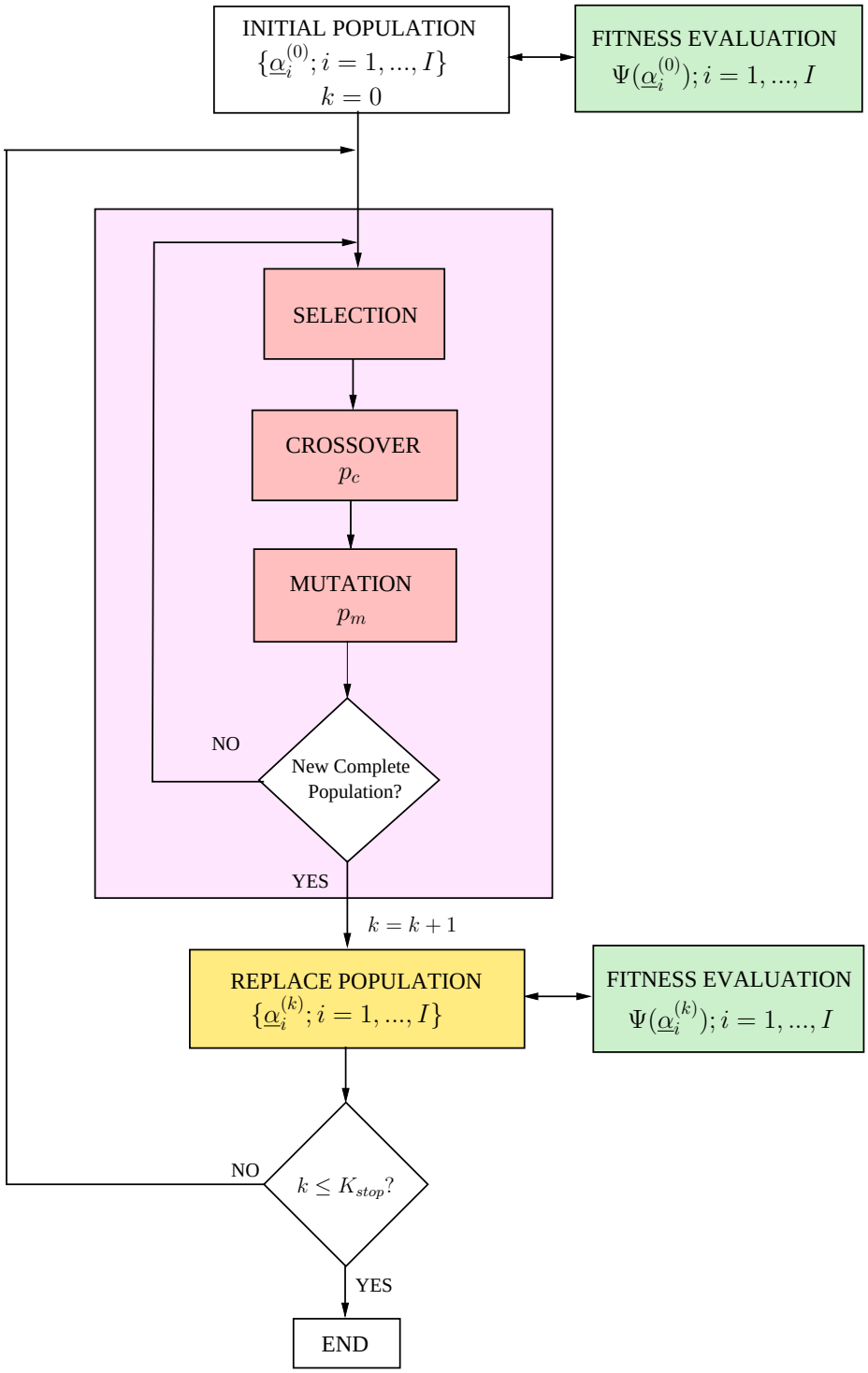

Fig. 2 - M. Salucci *et al.,* "Adaptive Nulling Through Subarray Switching ..."

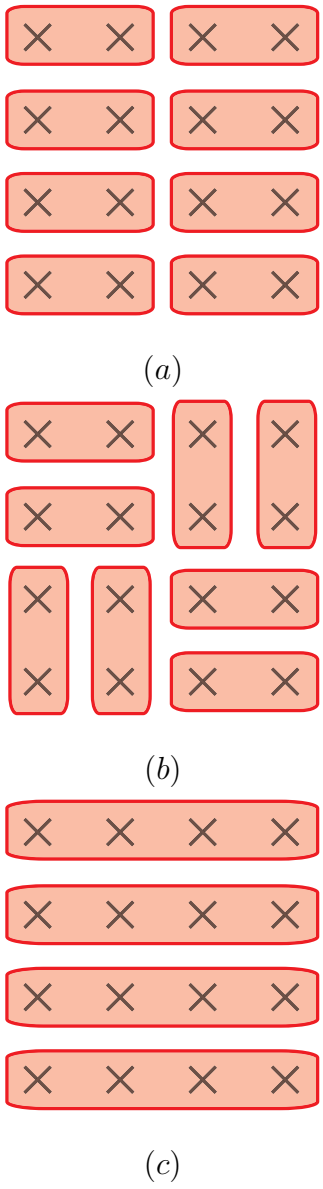

Fig. 3 - M. Salucci *et al.,* "Adaptive Nulling Through Subarray Switching ..."

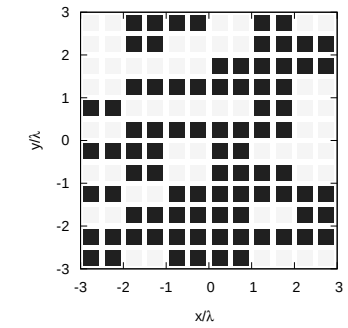

(a)

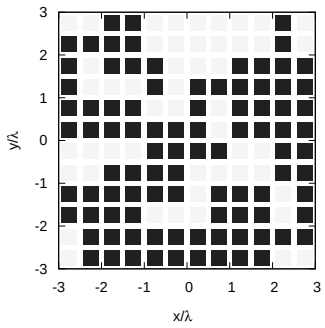

(c)

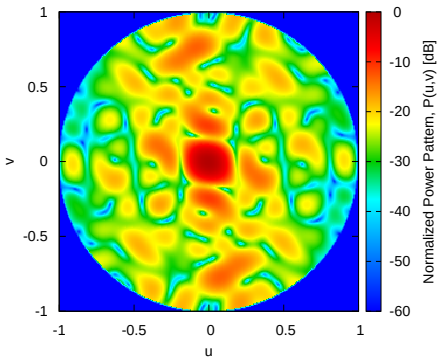

(b)

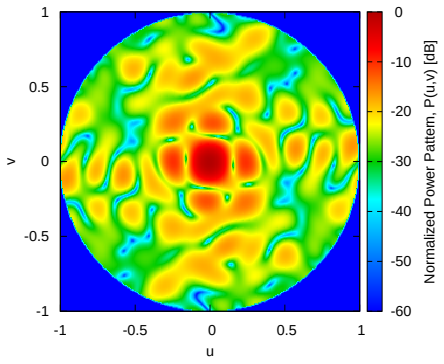

(d)

Fig. 4(*I*) - M. Salucci *et al.,* "Adaptive Nulling Through Subarray Switching ..."

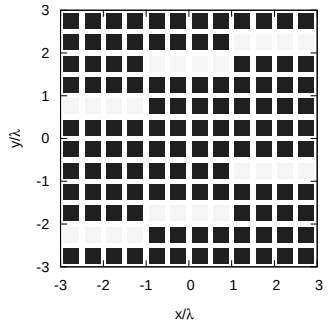

(e)

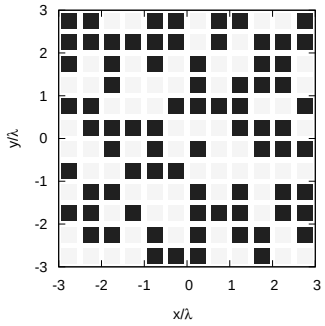

(g)

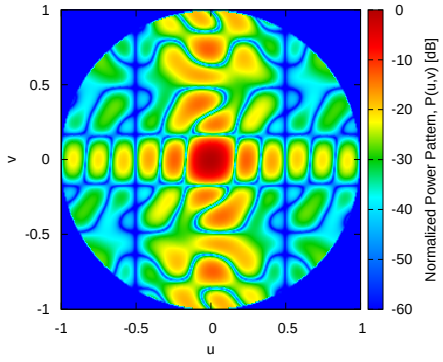

(f)

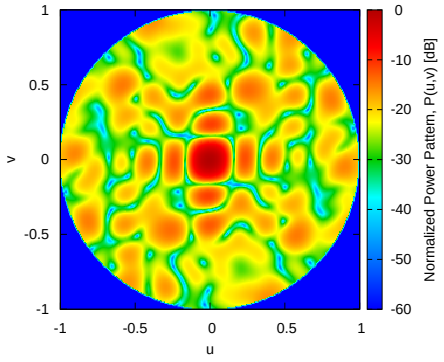

(h)

Fig. 4(*II*) - M. Salucci *et al.,* "Adaptive Nulling Through Subarray Switching ..."

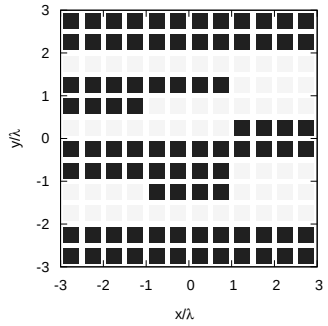

(e)

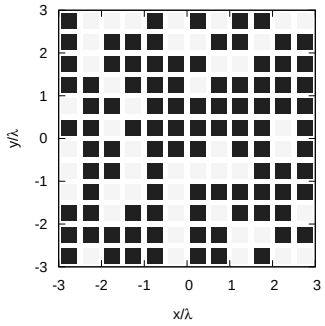

(g)

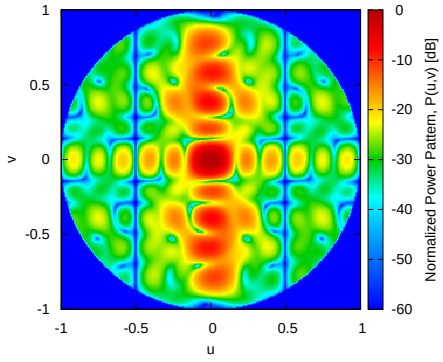

(f)

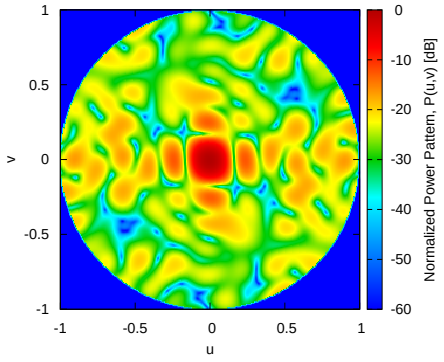

(h)

Fig. 5(*II*) - M. Salucci *et al.,* "Adaptive Nulling Through Subarray Switching ..."

	$avg\{\cdot\}$	$var\{\cdot\}$	$min\{\cdot\}$	$max\{\cdot\}$
	Q_2^H			
$SINR\,[dB]$	37.54	20.56	27.91	47.77
$\lvert AF(\theta_1,\phi_1)\rvert^2\ [dB]$	-68.24	31.02	-84.48	-57.94
	Q_2^{HV}			
$SINR\,[dB]$	47.05	6.52	35.67	49.57
$\lvert AF(\theta_1,\phi_1)\rvert^2\ [dB]$	-83.74	50.23	-105.27	-65.86
	Q_4			
$SINR\,[dB]$	31.62	40.63	20.56	50.77
$\lvert AF(\theta_1,\phi_1)\rvert^2\ [dB]$	-62.26	71.92	-104.10	-50.57
	Q_{full}			
$SINR\,[dB]$	40.01	13.71	33.44	47.81
$\lvert AF(\theta_1,\phi_1)\rvert^2\ [dB]$	-71.04	23.40	-84.05	-63.57

Tab. I - M. Salucci *et al.,* "Adaptive Nulling Through Subarray Switching ..."

	$avg\{\cdot\}$	$var\{\cdot\}$	$min\{\cdot\}$	$max\{\cdot\}$
	Q_2^H			
$SINR\,[dB]$	18.37	9.07	12.35	25.06
$\lvert AF(\theta_1,\phi_1)\rvert^2\ [dB]$	-51.78	18.77	-68.19	-45.45
$\lvert AF(\theta_2,\phi_2)\rvert^2\ [dB]$	-54.11	36.53	-69.04	-43.36
	Q_2^{HV}			
$SINR\,[dB]$	20.43	14.91	14.58	30.48
$\lvert AF(\theta_1,\phi_1)\rvert^2\ [dB]$	-54.86	31.00	-69.81	-46.70
$\lvert AF(\theta_2,\phi_2)\rvert^2\ [dB]$	-54.45	30.83	-68.94	-46.61
	Q_4			
$SINR\,[dB]$	18.41	10.46	12.75	28.33
$\lvert AF(\theta_1,\phi_1)\rvert^2\ [dB]$	-51.87	31.28	-67.91	-44.12
$\lvert AF(\theta_2,\phi_2)\rvert^2\ [dB]$	-54.15	31.70	-70.56	-43.91
	Q_{full}			
$SINR\,[dB]$	17.96	7.09	14.06	25.81
$\lvert AF(\theta_1,\phi_1)\rvert^2\ [dB]$	-52.61	29.17	-69.46	-44.85
$\lvert AF(\theta_2,\phi_2)\rvert^2\ [dB]$	-51.77	16.75	-65.99	-45.98

Tab. II - M. Salucci *et al.,* "Adaptive Nulling Through Subarray Switching ..."